Molecular Crystals and Liquid Crystals Science and Technology. Section A. Molecular Crystals and Liquid Crystals

Publication details, including instructions for authors and subscription information:
http://www.tandfonline.com/loi/gmcl19

Ensemble-Averaged Dynamic Light Scattering from Polymer-Stabilized Liquid Crystals

Pei-Yuan Liu [a], Alex M. Jamieson [a] & L. C. Chien [b]

[a] Macromolecular Science Department, Case Western Reserve University, Cleveland, OH, 44106-7202

[b] Liquid Crystal Institute, Kent State University, Kent, OH, 44242

Version of record first published: 24 Sep 2006

To cite this article: Pei-Yuan Liu, Alex M. Jamieson & L. C. Chien (2000): Ensemble-Averaged Dynamic Light Scattering from Polymer-Stabilized Liquid Crystals, Molecular Crystals and Liquid Crystals Science and Technology. Section A. Molecular Crystals and Liquid Crystals, 348:1, 187-205

To link to this article: http://dx.doi.org/10.1080/10587250008024806

Mol. Cryst. Liq. Cryst., Vol. 348, pp. 187-205
Reprints available directly from the publisher
Photocopying permitted by license only

Ensemble-Averaged Dynamic Light Scattering from Polymer-Stabilized Liquid Crystals

PEI-YUAN LIU[a], ALEX M. JAMIESON[a*] and L.C. CHIEN[b]

[a]*Macromolecular Science Department, Case Western Reserve University, Cleveland, OH 44106–7202 and* [b]*Liquid Crystal Institute, Kent State University, Kent, OH 44242*

(Received February 08, 1999; In final form September 24, 1999)

We report measurements of the viscoelastic parameters associated with the twist distortion of polymer-stabilized liquid crystal materials (PSLC), made by polymerizing 4,4′-bis-(acryloyloxy)-1,1′-biphenylene (BAB) and 4-butoxybenzyl 4-[6-(methacryloyloxyl-hexyloxy]benzoate (BMB6) to form fibrous networks in a nematic liquid crystal solvent (4′-phenyl-4-cyanobiphenyl, 5CB). By varying the BAB/BMB6 ratio, the twist elastic constant, K_{22}, and viscosity, γ_1, were investigated over a range of crosslink densities using electric-field-dependent dynamic light scattering (EFDLS). In PSLC samples, the formation of a highly-crosslinked, phase-separated polymer network can lead to optically heterogeneous behavior of the EFDLS data. Thus, it is necessary to evaluate the ensemble-averaged EFDLS relaxation function through spatial averaging. The results show that the polymer network causes a change in the twist relaxation rate, depending on the cross-link density of the specimens. The twist viscosity was found to increase with decrease in cross-link density, which appears to occur because higher cross-link density causes collapse of the gel fibers and less interaction between the fibers and nematic medium.

Keywords: Polymer stabilized liquid crystal; Heterogeneous medium; Phase separation.

INTRODUCTION

Thermally driven fluctuations of the orientational order in a nematic liquid crystal produce an intense depolarized Rayleigh scattering of light. The viscoelastic properties of nematic materials can be investigated by dynamic light scattering (DLS) analysis of this scattered light.[1–4] The appropriate theory was originally worked out by the Orsay group.[1] Of particular interest here is the scattering

* To whom all correspondence should be addressed.

geometry shown in Figure 1, in which the nematic director is aligned in the direction of propagation of the incoming light, the incident light is polarized perpendicular to the scattering plane, and depolarized scattered light is detected. For this situation, at small scattering angles, scattering from a pure twist distortion is observed, with a relaxation rate:[1]

$$\Gamma_2(q) = \frac{K_{22}q_\perp^2}{\gamma_1} \tag{1}$$

where K_{22} is the twist elastic constant; $\gamma_1$is the twist viscosity; and $q_\perp$ is the scattering vector perpendicular to the nematic director, $q_\perp = (2\pi n_e/\lambda)\sin\theta_0$ (where n_e is the temperature-dependent extraordinary refractive index of the nematic and θ_0 refers to the scattering angle inside the nematic sample). Since $q_\perp$ is known, we obtain the ratio of K_{22} to γ_1 which has the dimensions of a diffusion constant, and is referred to as the twist diffusivity. The individual values of the twist elastic constant (K_{22}) and viscosity coefficient (γ_1) can be obtained by carrying out the DLS measurements in the presence of an electric field applied parallel to the director (EFDLS). In this case, equation (1) becomes[2]

$$\Gamma_2(q) = \frac{K_{22}q_\perp^2}{\gamma_1} + \frac{\varepsilon_0\Delta\varepsilon\left(\frac{V}{d}\right)^2}{\gamma_1} \tag{2}$$

where $\Delta\varepsilon$ is the dielectric anisotropy of the liquid crystal; $\varepsilon_0$is the electric permittivity in vacuum; V is the applied voltage; and d is the cell thickness. It should be noted again that equation (2) is valid only at small scattering angles.[2,5,6]

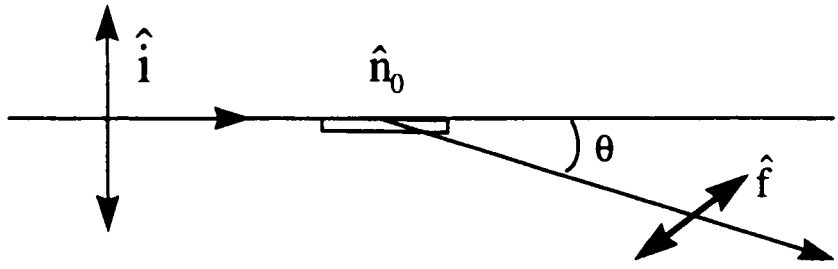

FIGURE 1 Scattering configuration in DLS measurement which selects twist and bend. Here $\hat{n}_0$ is the unit vector along the nematic director; θ is the scattering angle; and $\hat{i}$, $\hat{f}$ are polarization vectors for incoming and scattering light respectively

Recently, it has become of interest to extend this technique, which we have utilized for dilute solutions of a liquid crystal polymer in a nematic solvent,[5–8] to

determine the viscoelastic parameters of PSLC systems which are formed by *in situ* photopolymerization of reactive monomers in a nematic solvent. Here, as polymerization proceeds in the initially-homogeneous mixture to form a cross-linked gel network, phase separation occurs to form a spatially-heterogeneous material.[9] Moreover, one expects that the network elements will be swollen to some degree with a nematic solvent, and therefore one has an optically anisotropic network coexisting with a nematic solvent phase containing dissolved polymer. In contrast to a polymer solution, the polymer chains in a gel are localized by the cross-links to specific regions of the sample and are consequently able to execute only limited Brownian motions near fixed average positions. Therefore, a gel can be regarded as a restricted nonergodic medium since a localized area of a gel may be trapped in a limited region of the phase space.[10–15] For such media, the time-averaged intensity correlation function in a DLS measurement is no longer equal to the ensemble-averaged intensity correlation function, i.e. the average over a representative set of all possible spatial configurations. This means that a single DLS experiment does not provide an accurate estimate of the ensemble-average. This situation has been well-studied for isotropic gels and methods have been developed to extract dynamical parameters from such systems.[11–15] Pusey and Van Megen[10] pointed out that for nonergodic media, the ensemble-averaged correlation function can be obtained by spatial averaging of the DLS data from different areas within the sample. More recently, it was noted that[11–15] the total scattered intensity, $\langle I(q)\rangle_T$, of a gel consists of the sum of that from static inhomogeneities, $I_C(q)$, in the polymer network, and the dynamic component, $\langle I_F(q)\rangle_T$, from motion of the network, i.e., $\langle I(q)\rangle_T = I_C(q) + \langle I_F(q)\rangle_T$, where q is the magnitude of the scattering vector and $\langle\ldots\rangle_T$ denotes a time average value. Thus, the analysis of dynamic light scattering from heterogeneous media requires treatment of the heterodyne contribution between the static and dynamic components. This method of ensemble averaging has been referred to as the partial heterodyne technique.[11–15]

Light scattering has been applied recently to study dynamics of a liquid crystal dispersed in a glassy silica matrix,[16] in an aerogel host filled with nematic liquid crystal,[17,18] and polymer-dispersed liquid crystals.[19,20] The influence of surface, domain, and pore size was addressed. In dynamic light scattering study of such heterogeneous materials, nonergodic behavior, similar to that in isotropic gels, is expected,[18] but has not been characterized. In the present EFDLS study of polymer-stabilized liquid crystals, we indeed observe apparent non-ergodicity manifested by the fact that the depolarized time average scattered intensity, $\langle I(q)\rangle_T$, varies randomly with position in the highly cross-linked samples. In depolarized light scattering from such a PSLC specimen, we assume the spatial variation in EFDLS scattered intensity arises because, at a particular location, one is sam-

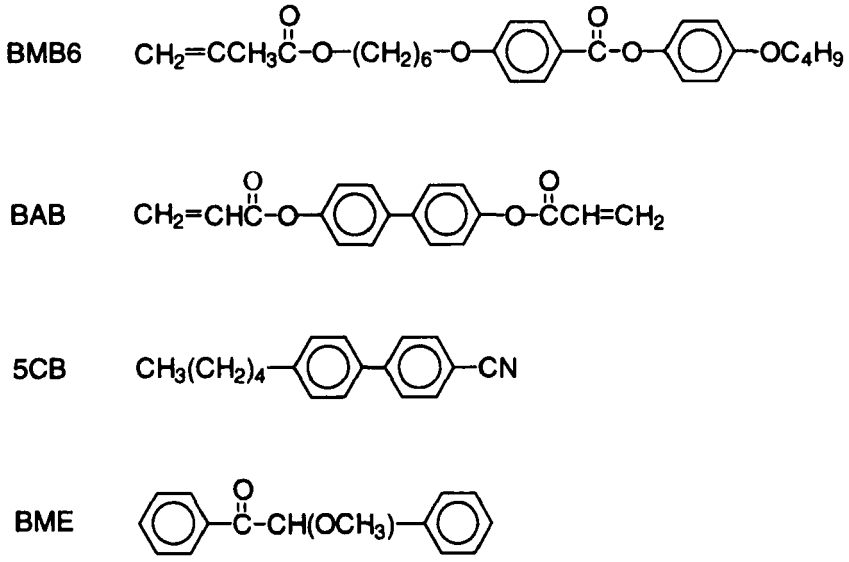

FIGURE 2 Chemical structures of PSLC constituents

pling a subset of the distribution of director orientation fluctuations. We assume the depolarized intensity is the sum of a static component from frozen director configurations and a dynamical component from twist fluctuations. Hence, we propose to apply the partial heterodyne ensemble-average method to EFDLS measurements to obtain reproducible information on the twist viscoelastic properties of highly cross-linked PSLC materials. We report EFDLS studies of PSLC mixtures having different cross-linked densities, formed by adjusting the ratio of bifunctional to monofunctional reactive monomers. By applying the partial heterodyne technique to the EFDLS data, we obtain data on the values of the twist viscosity coefficient (γ_1) and elastic constant (K_{22}) of a PSLC monodomain for different cross-linked densities.

EXPERIMENTAL

Samples were prepared by dissolving mixtures of 0.2wt% to 2.8 wt% of diacrylate monomer 4,4′-bis(acryloyloxy)-1,1-biphenylene (BAB), and 2.6 wt% to 0wt% of monofunctional monomer 4-butoxybenzyl 4-[6-(methacryloyloxy)-hexyloxy]benzate (BMB6), together with a double-bond-equimolar amount of the

photoinitiator, benzoin methyl ether (BME), into the nematic liquid crystal 4′-pentyl-4-cyanobiphenyl (5CB, purchased from BDH Ltd, T_{NI}=34.8 °C). All reagents were used as received. The structures of each species are shown in Figure 2. The bifunctional monomer (BAB), although not itself liquid crystal, is chemically similar to 5CB so that when a network forms, it is expected to have similar optical properties as the liquid crystal with some degree of orientational order. Table I shows the compositions and the phase transition temperatures of the PSLC specimens. The samples were heated to about 100 °C and ultrasonically agitated to make a homogeneous mixture. The cells, coated with indium tin oxide (ITO), and 0.5 wt% solution of lecithin in ethanol to induce homeotropic alignment, were filled with the reaction mixture in the isotropic phase at 40 °C using capillary action on a hot stage. Next, the samples were slowly cooled (2 °C/min) to the polymerization temperature (29.8 °C). The cell thickness was controlled by 12.5 μm Mylar spacers. The cells were sealed with epoxy resin (DEVCON). A Carl Zeiss optical polarizing microscope with a Mettler FP90 central processor and a Mettler FP82HT hot stage was utilized to determine the T_{NI} of the PSLC mixtures (see Table I) and assess the homogeneity and the homeotropic alignment of the samples.

TABLE I Compositions of PSLC specimens

Sample Name	*BAB (%, B)*	*BME (%)*	*BMB6 (%, M)*	*5CB %*	*T_{NI} (°C)[a]*
B28M0	2.80	0.46	0.00	96.74	30.9 – 31.6
0.5(B28M0)	1.40	0.23	0.00	98.37	31.8 – 32.2
B7M21	0.70	0.23	2.10	96.97	33.4 – 33.9
1.5 (B7M21)	1.05	0.35	3.15	95.44	33.4 – 33.6
B5M23	0.50	0.21	2.30	96.99	34.5 – 34.7
B2M26	0.20	0.17	2.60	97.03	34.8 – 34.9
5CB	0.00	0.00	0.00	100.00	34.8 – 35.0

Note:
1. In order to obtain the ensemble average data, each sample was measured at **50** different positions, except B5M23 and B2M26 which were measured at **5** positions.
2. Two different specimens of B28M0, B7M21, and 1.5(B7M21), and three different specimens of B5M23 and B2M26 were studied.

a. T_{NI} is the nematic to isotropic phase transition temperature at 2°C/min cooling rate.

Polymerization was initiated by UV radiation at wavelength λ=360 nm from a 100 Watt mercury spot lamp at 5 °C below the T_{NI} of the monomer mixtures, set by a temperature controller (YSI model 72) accurate to 0.2 °C, for approximately 30 min. All samples were cured at 15 volts in the presence of a 3000 Hz AC electric field with 1 mW/cm^2 UV light intensity, as monitored by a Cole-Parmer series 9811 radiometer during the photopolymerization process. The dielectric

anisotropy, $\Delta\varepsilon$ ($= \varepsilon_{//} - \varepsilon_{\perp}$), and the threshold voltage, V_{th}, of the PSLCs were determined via Freedericksz transition measurements described in detail elsewhere.[21] The value of $\varepsilon_{\perp}$ was measured at zero field or at voltages (with a 50 Hz AC bias voltage and an 1000 Hz probe signal) below the threshold in the planar cell and the value of $\varepsilon_{//}$ was obtained by measuring the capacitance of the homeotropic cell at a 7 volt in the presence of a 3000 Hz AC bias voltage frequency. For the EFDLS measurements, it is crucial to know the cell thickness d as indicated by equation (2). Briefly, the optical interference method using a He-Ne Laser and a microscope objective was applied to yield thickness values accurate to within 1%.[22] Also, the refractive indices of the PSLC samples were assumed to be equivalent to that of 5CB since the polymer concentrations used are very dilute.[8]

Dynamic light scattering experiments were performed with a photon correlation spectrometer consisting of a 15-mW He-Ne Laser and a Brookhaven Instruments BI-2030AT 264-channel digital correlator at a temperature of 29.8 °C. The samples were sandwiched between two glass slides and positioned in a refractive index-matched t-butylbenzene bath, thermostated to within ± 0.1 °C, using a custom-designed micromanipulator that enables a small adjustment to keep the scattering volume in the focal plane of the collecting lens. EFDLS measurements were typically made at a scattering angle of 18° in the laboratory frame. However, to confirm that the EFDLS decay rate at zero field follows the $q_{\perp}^2$ dependence predicted by equation (1), further measurements were made at additional angles between 12° and 21°. The depolarized intensity correlation functions of each specimen were obtained by data acquisition at either 5 or 50 different sample positions for each level of the AC electric field applied by a Hewlett-Packard audio-frequency generator model 200CDR at 3000 Hz. Since the twist mode is detected via depolarized scattering, this largely eliminates any stray isotropic scattering that could lead to a heterodyne component in the spectrum. To ascertain the level of static depolarized scattering, we heated the sample B28M0 above its T_{NI} and found that the average count rate decreased to ca. 1.2 % of the signal in the nematic phase. This observation indicates that any static component in the depolarized EFDLS scattering from the nematic state must originate in frozen director fluctuations. The detailed methodological procedures for EFDLS have been described elsewhere.[7] It should be noted that the normalized field correlation function of the depolarized scattered intensity, $g^{(1)}(\tau)$, obtained in the twist geometry shown in Figure 1, was analyzed by the cumulant method:

$$\ln g^{(1)}(\tau) = -\Gamma\tau + \frac{1}{2!}\mu_2\tau^2 + \cdots\cdots \tag{3}$$

where Γ is the mean decay rate, and μ_2 is the variance in the distribution of the decay rates. Typically, the normalized variance, μ_2/Γ^2, is small, of the order <

0.1, and independent of the electric field for homogeneous samples, but larger, in the range of 0.1 to 0.3, and generally decreasing with the electric field in the highly-crosslinked materials, 0.5(B28M0) and B28M0.

RESULTS AND DISCUSSION

PSLC specimens with various cross-linked densities were prepared having transition temperatures T_{NI} listed in Table I. The overall polymer content of all PSLC mixtures is 2.8% w/w of monomers, except for the specimen labeled 1.5(B7M21) for which the total concentration was increased by ×1.5, i.e. to 4.2 % w/w, and for the sample named 0.5(B28M0) for which there was a 50 % decrease of the polymer concentration from 2.8 to 1.4 wt%. The values of $\Delta\varepsilon$ and V_{th} from the Freedericksz transition experiment for all samples prior to and after photo-initiated polymerization are shown in Table II. Essentially, we find, in agreement with Mora *et al.*,[23] that $\Delta\varepsilon$ of the PSLC samples before polymerization is not distinguishable from that in pure 5CB. After the monomer-initiator-5CB mixtures were photopolymerized in the nematic state in the field-on condition for the homeotropic cell and the field-off condition for the planar cell, the $\Delta\varepsilon$ values of the PSLC specimens are slightly lower and the V_{th} values are slightly higher, indicating that a decrease in the local order parameter has occurred. This phenomenon was also observed by Crawford *et al.*[24] who further noted that, in the absence of the electric field, the orientation of the nematic director is no longer fixed by the anchoring force from the substrate, but by the polymer network. It is expected that the network photopolymerized in the presence of an electric field ought to be highly anisotropic, with its fibers aligned along the direction of nematic order. However, the polymerization process in a highly-crosslinked polymer network is not uniform, and local disorientation, relative to the nematic director, is produced on a variety of length scales.[25] These nematic PSLC gels exhibit different textures as assessed by optical examination in the cross-polarizing microscope. For example, B28M0 as well as 0.5(B28M0) sample shows speckles on the micron scale, as evident in Figure 3, indicating extensive phase separation, whereas the viewfield of other specimens (B7M21, B5M23, and B2M26) like 5CB in Figure 3 is uniformly dark, indicating that the homeotropic alignment is largely preserved throughout the sample in the absence of the electric field for ratios of monofunctional to bifunctional monomer M/B ≥ 3.

In photon correlation spectroscopy of spatially inhomogeneous gel materials which contain quasi-static random refractive index fluctuations, the time average scattered intensity, $\langle I(q)\rangle_T$, becomes sample-position dependent, leading to the appearance of a speckle pattern. Consequently, the $\langle I(q)\rangle_T$ value, measured at

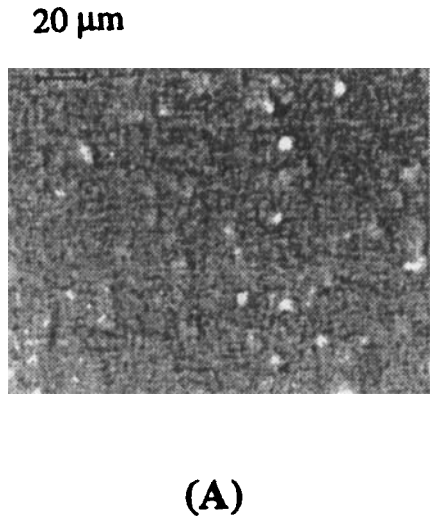

FIGURE 3 Cross-polarizing optical micrographs of PSLC film obtained via photopolymerization of monomer mixtures in 5CB in the nematic state at 29.8°C in the presence of a 15 volt 3000 Hz AC electric field: (A) B28M0 specimen; (B) Pure 5CB

different positions in such samples, displays an enormous variation, indicating that miscellaneous sub-ensembles of the scattering properties are detected. This situation is indeed observed in PSLC gels as evident in Figure 4 which shows the

depolarized EFDLS speckle patterns recorded at $\theta = 18°$ on specimens of 5CB, B7M21, and B28M0 in the absence of an applied electric field. In this case, fifty different positions within the sample were chosen at random, and the time average scattered intensity, $\langle I(q)\rangle_T$, was determined at each sample position by adjusting the micromanipulator laterally with respect to the incoming monochromatic light. The dotted lines in these figures represent the ensemble average values, $\langle I(q)\rangle_E$, determined as the average over the individual spatially-varying records. It is apparent, as indicated in Figure 4, that the fluctuation in $\langle I(q)\rangle_T$ and the value of $\langle I(q)\rangle_E$ increases for sample B28M0 which has a higher cross-link density, because of the increased inhomogeneity of the polymer network. In contrast, the $\langle I(q)\rangle_E$ value of sample B7M21 which has a low cross-link density is numerically comparable to the $\langle I(q)\rangle_E$ value of pure 5CB. As shown in Figure 5, when B28M0 is subjected to an applied 3000 Hz AC electric field of 8 and 20 volts at scattering angle 18°, the spatial inhomogeneities are increasingly suppressed by the field, and the time average scattered intensity, $\langle I(q)\rangle_T$, decreases, as expected on theoretical grounds.[2]

While the analysis of Pusey and Van Megen[10] refers to isotropic scattering from sub-ensembles of the relaxation spectrum of concentration fluctuations, in depolarized EFDLS scattering from PSLC gels, we are sampling a subset of the distribution of relaxation times for director reorientation. Consistent with this interpretation, the spatial variation of the EFDLS relaxation rates is found to be larger for samples with higher cross-linked densities. To quantitatively interpret EFDLS data from PSLC gels in the twist geometry, however, we need to take into account the heterogeneity of gels by carrying out an ensemble average DLS[10,12,15] analysis. For each speckle, the normalized intensity-intensity time correlation function, $g^{(2)}(\tau)$, was well fitted via the cumulant method (equation (3)) in the form:

$$g^{(2)}(\tau) = 1 + \alpha\sigma_I^2\left|g^{(1)}(\tau)\right|^2 = 1 + \alpha\sigma_I^2 \exp[-2D_A q_\perp^2 \tau + \mu_2\tau^2] \qquad (4)$$

where D_A is the apparent twist diffusivity; α is the instrumental coherence factor ($0 < \alpha < 1$); and σ_I^2 represents the initial amplitude of $g^{(2)}(\tau)$.

We adopt the partial heterodyne analysis procedure, proposed by Joosten et al.,[12] by means of which the mean value of the twist diffusivity, D, and the time-averaged value of the light scattering intensity from the liquid-like twist fluctuations, $\langle I_F(q)\rangle_T$, of a heterogeneous specimen can be estimated by a least squares fit of a plot of D_A versus $\langle I(q)\rangle_T$ using the following equation:

$$D_A = \frac{D}{2 - X} = \frac{D}{2 - \langle I_F(q)\rangle_T / \langle I(q)\rangle_T} \qquad (5)$$

where $X = \dfrac{\langle I_F(q)\rangle_T}{\langle I(q)\rangle_T}$

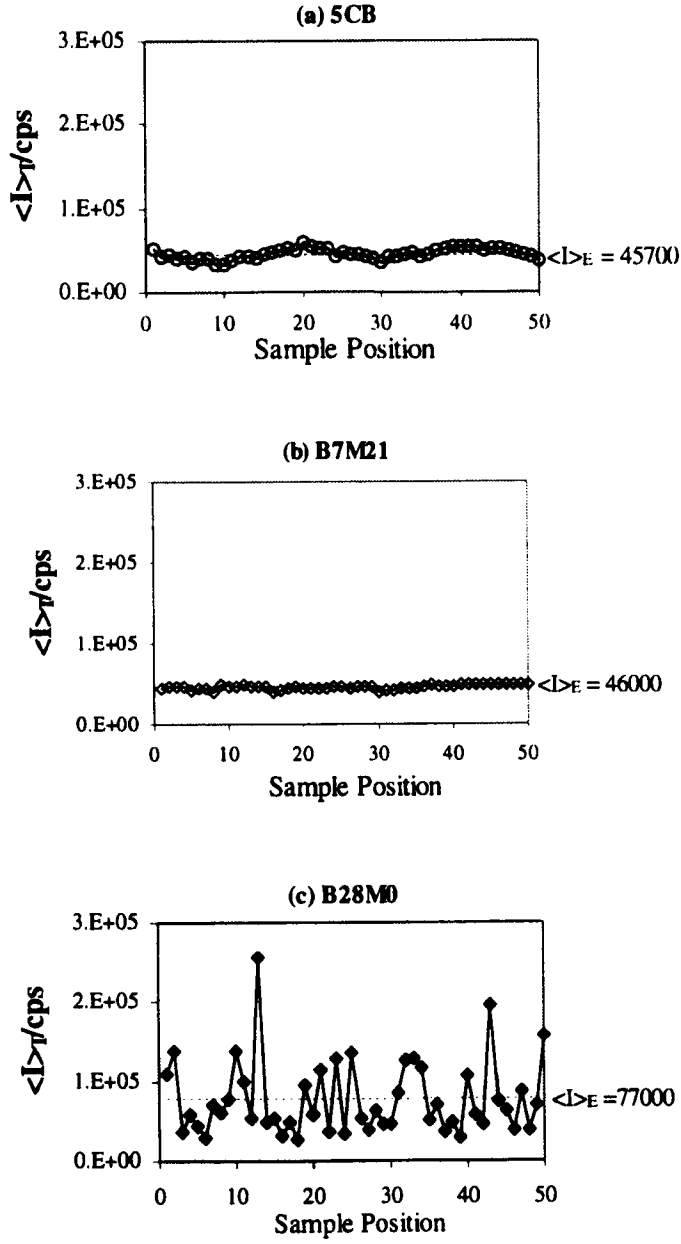

FIGURE 4 Spatial variation of time averaged scattered intensity, $\langle I(q)\rangle_T$, for (a) 5CB; (b) B7M21; and (c) B28M0 specimens in the field-off condition. $\langle I\rangle_E$ represents the ensemble-averaged scattered intensity

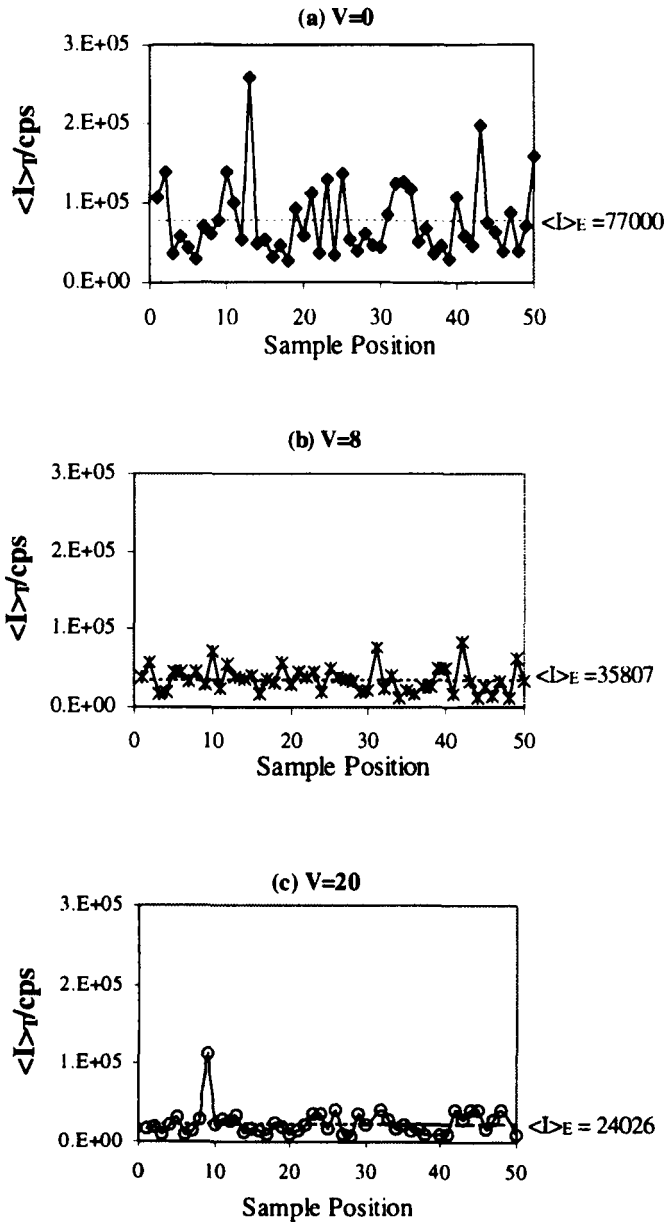

FIGURE 5 Spatial variation of EFDLS time averaged scattered intensity, $\langle I(q)\rangle_T$, for B28M0 PSLC specimen. $\langle I\rangle_E$ represents the ensemble-averaged scattered intensity: (a) applied voltage = 0V; (b) applied voltage = 8V; (c) applied voltage = 20V

TABLE II Dielectric anisotropies (Δε) of PSLC specimens

	B28M0	*0.5(B28M0)*	*B7M21*	*1.5(B7M21)*	*B5M23*	*B2M26*	*5(*
$\Delta\varepsilon = \varepsilon_{\parallel}^{H} - \varepsilon_{\perp}^{P}$	11.39	11.29	11.32	11.23	11.07	11.35	11.
V_{th}	0.70	0.68	0.68	0.69	0.68	0.68	0.(
$\Delta\varepsilon = \varepsilon_{\parallel}^{H} - \varepsilon_{\perp}^{P}$	10.64	10.59	10.56	10.67	10.24	11.20	–
V_{th}	0.75	0.75	0.70	0.70	0.71	0.70	–

ericksz transition threshold voltage.

epresent, respectively, values of the dielectric constant parallel and perpendicular to the director measured in homeotropic and planar c

For a heterogeneous medium, D_A varies with sample position between the limits 0 (pure heterodyne) < × < 1 (pure homodyne), i.e., D/2 < D_A < D. Equation (5) can be rewritten in the form:[14,15]

$$\frac{< I(q) >_T}{D_A} = \frac{2}{D} < I(q) >_T - \frac{< I_F(q) >_T}{D} \tag{6}$$

Hence, D and $<I_F(q)>_T$ can be determined by carrying out a linear plot of $<I(q)>_T/D_A$ vs. $<I(q)>_T$. Figure 6 shows D_A and $<I(q)>_T/D_A$, respectively, plotted as a function of $<I(q)>_T$ together with least squares fits to equations (5) and (6). As evident in Figure 6, the dynamic light scattering from the heterogeneous material B28M0 is well-described by the partial heterodyne analysis. Comparable fits were obtained in the absence and presence of the applied electric field.

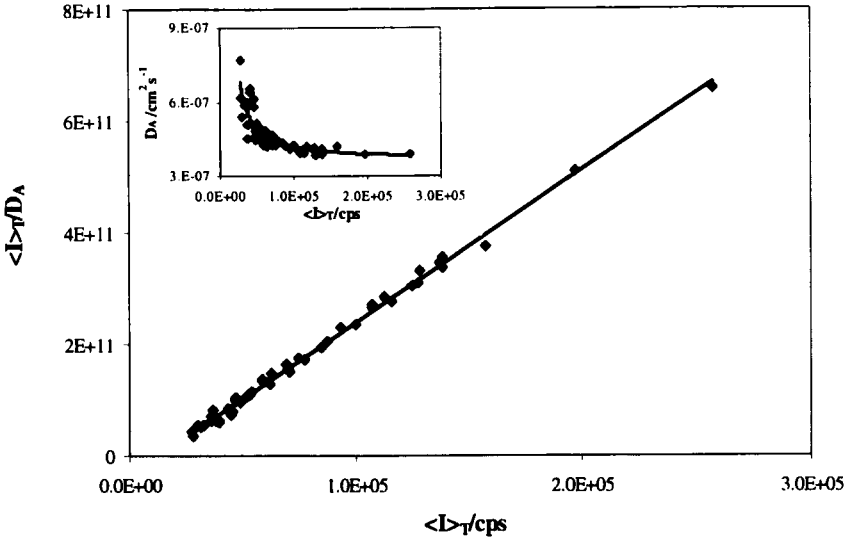

FIGURE 6 Plot of $<I>_T/D_A$ vs. $<I>_T$ for highly cross-linked material B28M0 in the absence of an electric field. The straight line indicates the fit to equation (6). The inset shows the corresponding plot according to equation (5)

Accordingly, for the fully cross-linked PSLC specimens B28M0 and 0.5(B28M0), the relaxation rates Γ_2 of the twist mode and associated twist diffusivities D were derived via equation (6). Samples of low cross-link density, B7M21, B5M23, and B2M26, were found to exhibit homogeneous behavior comparable to that of pure 5CB, and hence the ensemble-averaged relaxation rates $<\Gamma_2>_E$ were determined as the mean of the individual positional decay rates. We list in Table III the measured values of the relaxation rates, Γ_2, and the

time-average scattering intensity from the liquid-like twist fluctuations, $\langle I_F(q)\rangle_T$, derived by partial heterodyne analysis for samples B28M0 and 0.5(B28M0) at each field strength. Note that subscripts PH1 and PH2 represent, respectively, two independent samples of B28M0, analyzed by the partial heterodyne (PH) method. These duplicate experiments were performed with different cells to investigate the reproducibility of the data.

TABLE III Partial heterodyne analysis of field dependent EFDLS relaxation rates, Γ_2, and the time-average scattering intensity from the liquid-like fluctuations, $\langle I_F(q)\rangle_T$, for PSLC materials 0.5(B28M0) and B28M0 (d = measured cell thickness)

Sample Name		*V = 0*	*V = 4*	*V = 8*	*V = 12*	*V = 16*	*V = 20*
$\langle$0.5(B28M0)$\rangle_{PH}$ (d = 22μm)	Γ_2 (± 2%)	1280	1293	1445	1680	2067	2688
	$\langle I_F\rangle_T$ (± 6%)	26578	23838	22021	18483	14779	8764
$\langle$B28M0$\rangle_{PH1}$ (d = 15μm)	Γ_2 (± 1.5%)	1541	1647	2088	2800	3846	5218
	$\langle I_F\rangle_T$ (± 6%)	23767	18939	13843	10535	9247	7697
$\langle$B28M0$\rangle_{PH2}$ (d = 19μm)	Γ_2 (± 1%)	1525	1603	1884	2331	3015	3739
	$\langle I_F\rangle_T$ (± 7%)	18542	18794	15442	13327	9540	11921

First, the dependence on $q_\perp^2$ of the DLS twist relaxation mode of B28M0 in the absence of the electric field is shown in Figure 7. The scattering angles in this experiment range from 12° to 21° in steps of 3°. At each angle, the time-averaged DLS relaxation rate was obtained at 50 different positions within a highly phase-separated specimen B28M0 and analyzed by the partial heterodyne method to obtain the twist relaxation rate. In agreement with equation (1), the twist relaxation frequency exhibits $q_\perp^2$ dependence, and goes to zero as $q_\perp^2 \to 0$, with coefficient of variance (C.V.) values of 2 % at each angle, as indicated in Figure 7. In further agreement with theory, as shown in Figure 8, the relaxation rates of the twist mode obtained by partial heterodyne analysis are found to increase linearly with the electric field parameter $\varepsilon_0\Delta\varepsilon(V/d)^2$. Also, as shown in Table III, the liquid-like scattering intensity $\langle I_F(q)\rangle_T$ decreases with increase of the electric field parameter, reflecting a decrease in the amplitude of the liquid-like director fluctuations. It is relevant to note that $\langle I_F(q)\rangle_T$ at V = 0 is substantially smaller than the scattering intensity from pure 5CB (Figure 4(a)). This may be due to the segregation which occurs on cross-linking such that one is measuring the scattering from polymer-poor microdomains within the scattering volume. From the plot of Figure 8, the values of K_{22} and γ_1 can be determined, respectively, from the intercept and the reciprocal of the slope via a least squares fit to equation (2). The results are listed in Table IV.

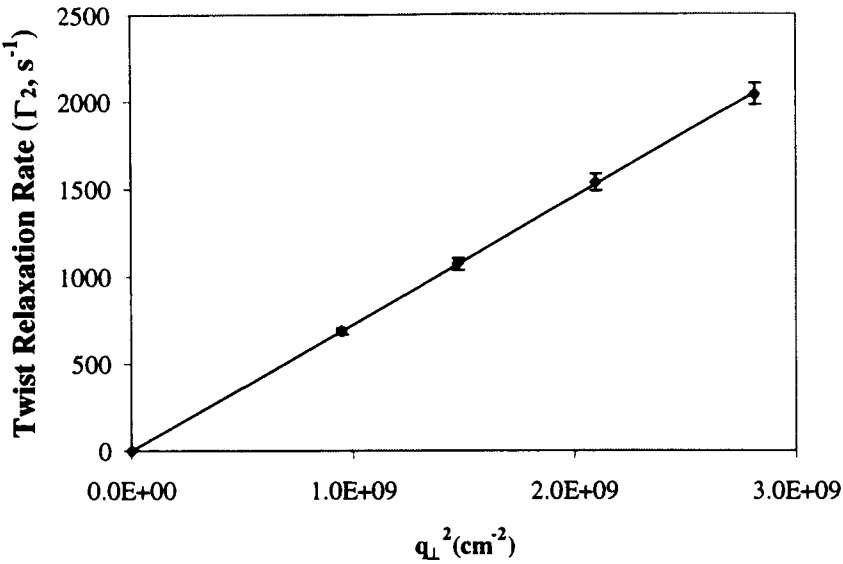

FIGURE 7 Spatial variation of DLS twist relaxation rate as a function of $q_\perp^2$ for B28M0 PSLC specimen

TABLE IV Ensemble averaged values of the percent increase in twist viscosity $\Delta\gamma_1/\gamma_1^0$ and elastic constants $\Delta K_{22}/K_{22}^0$ of PSLC materials

Sample Name	$\Delta\varepsilon \pm 1\%$	$V_{th} \pm 2\%$ *(Volts)*	$\gamma_1 \pm 6\%$ *(poise)*	$\Delta\gamma_1/\gamma_1^0$	$K_{22} \pm 6\%$ *(10^{-7}dynes)*	$\Delta K_{22}/K_{22}^0$
$\langle 5CB\rangle_E$	11.17	0.69	0.54	–	3.26	–
$\langle 0.5(B28M0)\rangle_{PH}$	10.59	0.75	0.53	–0.02	3.13	–0.04
$\langle B28M0\rangle_{PH1}$	10.64	0.75	0.46	–0.15	3.30	0.01
$\langle B28M0\rangle_{PH2}$	10.64	0.75	0.48	–0.11	3.52	0.08
$\langle B7M21\rangle_{E1}$	10.56	0.70	0.87	0.61	2.46	–0.25
$\langle B7M21\rangle_{E2}$	10.56	0.70	0.90	0.67	2.71	–0.17
$\langle 1.5(B7M21)\rangle_{E1}$	10.67	0.70	4.01	6.43	3.20	–0.02
$\langle 1.5(B7M21)\rangle_{E2}$	10.67	0.70	3.98	6.37	3.06	–0.06
$\langle B5M23\rangle_5$	10.24	0.71	1.01	0.87	3.68	0.13
$\langle B2M26\rangle_5$	11.20	0.70	0.81	0.50	3.76	0.15

We note from Table IV that the ensemble-averaged values of γ_1 and K_{22}, derived from measurement series PH1 and El, for specimens B28M0, B7M21, or

1.5(B7M21) by equation (2) are in good agreement with the values obtained from measurement series PH2 and E2 to within 6 % relative error. Thus, the reproducibility for each of these three samples is very good. Next, the results in Table IV indicate that the formation of a polymer network in 5CB causes a change in both the twist viscosity coefficient and the twist elastic constant, combining to produce a change in mean decay rate. To study and compare the effect of variation in crosslinked density of the polymer network, we further list in Table IV values of the percent increase in twist viscosity $\Delta\gamma_1/\gamma_1{}^0 = (\gamma_1 - \gamma_1{}^0)/\gamma_1{}^0$, and, likewise, values of the percent increase of twist elastic constant $\Delta K_{22}/K_{22}{}^0 = (K_{22}-K_{22}{}^0)/K_{22}{}^0$, where $\gamma_1{}^o$ and $K_{22}{}^o$ are the twist viscosity coefficient and elastic constant of pure 5CB. The changes in $\Delta K_{22}/K_{22}{}^0$ for all samples are comparatively small, and exhibit no particular trend with cross-link density or polymer concentration. The change in $\Delta\gamma_1/\gamma_1{}^0$ varies strongly with cross-link density, such that $\Delta\gamma_1/\gamma_1{}^0$ for highly cross-linked materials, 0.5(B28M0) and B28M0, is negative and substantially smaller than for the samples with low cross-linked densities, for which $\Delta\gamma_1/\gamma_1{}^0$ is large and positive.

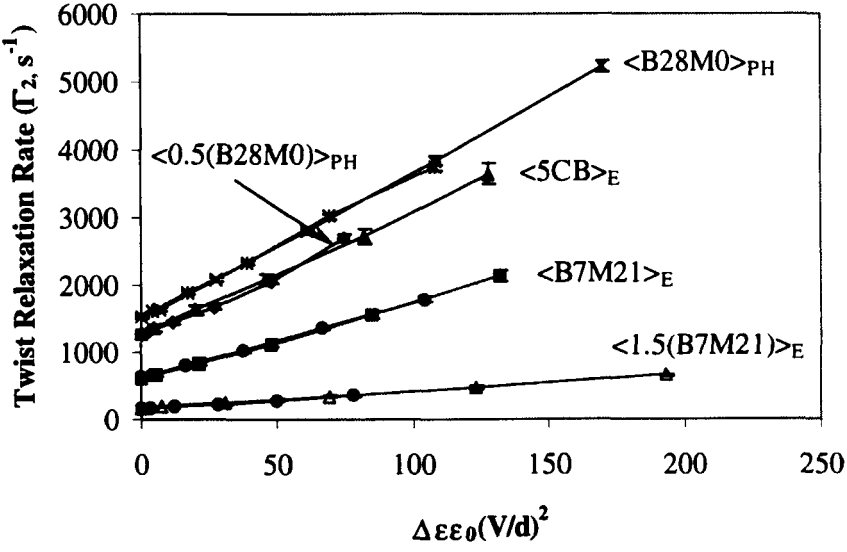

FIGURE 8 Dependence of the twist decay rate on the applied voltage for various PSLC specimens

The effect of the polymer concentration at fixed cross-link density on the percent increase of twist viscosity coefficient was examined. As evident in Figure 8 and Table IV, variation of polymer concentration has an opposite effect, when comparing the highly cross-linked specimens, 0.5(B28M0) and B28M0, versus

the less cross-linked samples, B7M21 and 1.5(B7M21). In the case of the fully cross-linked PSLCs, $\Delta\gamma_1/\gamma_1{}^0$ of B28M0 decreases only slightly with an increase of the polymer concentration from 0 to 2.8 wt% and, indeed, for 0.5(B28M0), which has polymer concentration 1.4 wt%, $\Delta\gamma_1 \sim 0$, i.e. the twist viscosity is the same as that of pure 5CB within experimental error. In contrast, for the less cross-linked specimens, an increase of the polymer concentration (from 2.8 to 4.2 wt%) results in a very large increase in the twist viscosity coefficients, as shown in Table IV. Specifically, $\Delta\gamma_1/\gamma_1{}^0$ of 1.5(B7M21) is approximately 10 times that of B7M21.

In the highly cross-linked samples, the polymer network has a negligible viscous interaction with the solvent. In the lightly cross-linked samples, a very large interaction occurs. The distinct behavior of the highly cross-linked samples versus those of low cross-link density correlates with a morphological evolution from heterogeneous phase-separated gels to homogeneous materials. The dynamical behavior can be qualitatively understood within the context of a theoretical analysis by Brochard,[26] using the Landau-DeGennes expansion of the free energy of swelling of an isotropic network in a nematogenic solvent. Once such a gel is immersed in a nematic solvent, the configuration of the chains becomes anisotropic. Osmotic swelling pressures compete with elastic restoring forces to determine the equilibrium state. When nematic order appears in the pure solvent, the chemical potential of the solvent outside the gel drops to a level lower than that inside the gel, from which it follows that solvent must be expelled from the gel. Under this condition, to balance the presence of the nematic order, a higher osmotic pressure is required inside the gel and the gel collapses into a dense state. Since the elastic restoring force increases with cross-link density, collapse is favored by a decrease in N, the number of chain statistical segments between cross-links. Additionally, the analysis of Brochard predicts[26] a reduction of the transition temperature inside the gel, which behavior is indeed consistent with our observation that the onset of T_{NI}occurs at a lower temperature for the highly-crosslinked density specimens, 0.5(B28M0) and B28M0. Similar conclusions were drawn by Ballauff[27] who observed that, below T_{NI}, the network shrinks to a size scale scarcely exceeding the dimensions in the dry state, reflecting a strong demixing tendency of the polymer gel and nematic solvent upon formation of an ordered phase. The above observations are also consistent with the structural model of PSLC materials developed by Crawford *et al.*,[24,28] who deduced that B28M0 consists of polymer fibrils with nanometre-scale radii, surrounded by thin layers of liquid crystal, aggregated into fiber bundles separated by polymer-poor 5CB regions. In consequence, a substantial volume of pure nematic, under the anisotropic effect of the surrounding network fibrils, can relax quickly, which leads to a higher twist relaxation rate and lower $\Delta\gamma_1/\gamma_1{}^0$, in con-

trast to samples B7M21, B5M23, and B2M26 with more swollen polymer networks.

Under these conditions, for a highly-crosslinked gel, it seems reasonable that K_{22} and γ_1 will have values relatively close to that of the pure solvent, as found experimentally. Specimens having lower cross-linked densities will be more swollen by the nematic solvent and hence are expected to have a large increase in γ_1 because of hydrodynamic interactions between polymer and solvent. It is interesting that the γ_1 values of the highly cross-linked B28M0 specimens appear to be slightly smaller than that of the pure solvent 5CB. This may reflect a decrease in the order parameter of the nematic solvent due to the interaction with the network fibers.[24]

CONCLUSIONS

Electric field-dependent dynamic light scattering from anisotropic PSLC networks over a range of different crosslink densities was investigated. The photopolymerization of the gels in the nematic state in the presence of an electric field, at 2.8wt% of polymer concentration, produces heterogeneous PSLC materials, when the monomer feed ratio of [BMB6]/[BAB] (g/g) is smaller than 3 as evidenced, via microscopic examination. By determining the partial heterodyne ensemble-averaged twist relaxation rates in EFDLS experiments, reproducible average values of the twist viscosity γ_1 and elastic constant K_{22} can be obtained for such phase-separated PSLC samples within 6% relative error. The presence of the polymer network produces a change in twist viscosity which is larger for less cross-linked materials. This appears to occur because of an increased tendency for demixing of the polymer network at higher cross-link densities, and therefore less hydrodynamic interaction between the polymer and the solvent.

Acknowledgements

We thank Mr. Doug Bryant at Kent State University for preparation of polyimide-coated and ITO-coated glass slides, and a reviewer for useful comments. This work was supported by a grant from the National Science Foundation Science and Technology Center ALCOM, DMR 89–20147.

References

(1) Orsay Liquid Crystal Group, *J. Chem. Phys.*, **51**, 816 (1969).
(2) F.M. Leslie, and C.M. Waters, *Mol. Cryst. Liq. Cryst.*, **123**, 101 (1985).
(3) M.S. Sefton, A.R. Bowdler, and H.J. Coles, *Mol. Cryst. Liq. Cryst.*, **129**, 1 (1985).
(4) P.G. De Gennes, and J. Prost, *The Physics of Liquid Crystals* (Claredon Press: Oxford, 1993), 2nd Ed.

(5) F.L. Chen and A.M. Jamieson, *Macromolecules*, **27**, 1943 (1994).
(6) F.L. Chen, A.M. Jamieson, M. Kawasumi, and V. Percec, *J. Polym. Sci., Polym. Phys.*, **33**, 1213 (1995).
(7) D. Gu, A.M. Jamieson, C. Rosenblatt, D. Tomazos, M. Lee, and V. Percec, *Macromolecules*, **24**, 2385 (1991).
(8) D. Gu, A.M. Jamieson, M. Lee, M. Kawasumi, and V. Percec, *Macromolecules*, **25**, 2151 (1992).
(9) A. Jakli, L. Rosta, and L. Noirez, *Liquid Crystals*, **18**, 601 (1995).
(10) P.N. Pusey, and W. Van Megen, *Physica A*, **157**, 705 (1989).
(11) S. Mallam, F. Horkay, A.M. Hecht, E. Geissler, *Macromolecules.*, **22**, 3356 (1989).
(12) J.G.H. Joosten, J.L. McCarthy, P.N. Pusey, *Macromolecules*, **24**, 6690 (1991).
(13) L. Fang, and W. Brown, *Macromolecules*, **25**, 6897 (1992).
(14) M. Shibayama, *Macromol. Chem. Phys.*, **199**, 1 (1998).
(15) M. Shibayama, T. Norisuye, S. Nomura, *Macromolecules.*, **29**, 8746 (1996).
(16) X.-L. Wu, W.I. Goldburg, M.X. Liu, and J.Z. Xue, *Phys. Rev. Lett.*, **69**, 470 (1992).
(17) A. Mertelj and M. Čopič, *Phys. Rev. E*, **55**, 504 (1997).
(18) T. Bellini, N.A. Clark, and D.W. Schaefer, *Phys. Rev. Lett.*, **74**, 2740 (1995).
(19) A. Mertelj, L. Spindler, and M. Čopič, *Phys. Rev. E*, **56**, 549 (1997).
(20) P. Allia, C. Oldano, M. Rajteri, P. Taverna, L. Trossi, and R. Aloe, *Liquid Crystals*, **18**, 555 (1994).
(21) D. Gu, S.R. Smith, A.M. Jamieson, M. Lee, and V Percec, *J Phys. II (France)*, **3**, 937 (1993).
(22) F.L. Chen, *Ph.D. Thesis*, Case Western Reserve University, Cleveland, OH (1994).
(23) S. Mora, A.M. Jamieson, and L.C. Chien, *Mol. Cryst. Liq. Cryst.*, **292**, 323 (1997).
(24) G.P. Crawford, A. Scharkowski, Y.K. Fung, J.W. Doane, And S. Zumer, *Phys. Rev. E.*, **52**, R1273 (1995).
(25) C.C. Chang, L.C. Chien, and R.B. Meyer, *Phys. Rev. E.*, **56**, 595 (1997).
(26) F. Brochard, *J. Physique*, **40**, 1049 (1979).
(27) M. Ballauff, *Mol. Cryst. Liq. Cryst.*, **196**, 47 (1991).
(28) S. Zumer and G.P. Crawford, *Liquid Crystals in Complex Geometries: formed by polymer and porous networks* (Taylor and Francis, London, 1996), G.P. Crawford, S. Zumer Eds.